ARTICLE

Anaplastic lymphoma kinase-positive anaplastic large cell lymphoma with the variant RNF213-, ATIC- and TPM3-ALK fusions is characterized by copy number gain of the rearranged ALK gene

Jo-Anne van der Krogt,[1,*] Marlies Vanden Bempt,[1,2,*] Julio Finalet Ferreiro,[1] Nicole Mentens,[1,2] Kris Jacobs,[1,2] Ursula Pluys,[1] Kathleen Doms,[1] Ellen Geerdens,[1,2] Anne Uyttebroeck,[3] Pascal Pierre,[4] Lucienne Michaux,[1] Timothy Devos,[5] Peter Vandenberghe,[1,5] Thomas Tousseyn,[6,7] Jan Cools[1,2] and Iwona Wlodarska[1]

*JAvdK and MVB contributed equally to this work

[1]Center for Human Genetics, KU Leuven; [2]Center for Cancer Biology, VIB, Leuven; [3]Department of Pediatrics, University Hospitals Leuven; [4]Department of Hematology, Cliniques Sud Luxembourg, Arlon; [5]Department of Hematology, University Hospitals Leuven; [6]Translational Cell and Tissue Research KU Leuven and [7]Department of Pathology, University Hospitals Leuven, Belgium

EUROPEAN HEMATOLOGY ASSOCIATION

Ferrata Storti Foundation

Haematologica 2017
Volume 102(9):1605-1616

ABSTRACT

Anaplastic lymphoma kinase (ALK)-positive anaplastic large cell lymphoma is characterized by 2p23/*ALK* aberrations, including the classic t(2;5)(p23;q35)/*NPM1-ALK* rearrangement present in ~80% of cases and several variant t(2p23/ALK) occurring in the remaining cases. The *ALK* fusion partners play a key role in the constitutive activation of the chimeric protein and its subcellular localization. Using various molecular technologies, we have characterized ALK fusions in eight recently diagnosed anaplastic large cell lymphoma cases with cytoplasmic-only ALK expression. The identified partner genes included *EEF1G* (one case), *RNF213/ALO17* (one case), *ATIC* (four cases) and *TPM3* (two cases). Notably, all cases showed copy number gain of the rearranged *ALK* gene, which is never observed in *NPM1-ALK*-positive lymphomas. We hypothesized that this could be due to lower expression levels and/or lower oncogenic potential of the variant *ALK* fusions. Indeed, all partner genes, except *EEF1G*, showed lower expression in normal and malignant T cells, in comparison with *NPM1*. In addition, we investigated the transformation potential of endogenous Npm1-Alk and Atic-Alk fusions generated by clustered regularly interspaced short palindromic repeats/Cas9 genome editing in Ba/F3 cells. We found that Npm1-Alk has a stronger transformation potential than Atic-Alk, and we observed a subclonal gain of *Atic-Alk* after a longer culture period, which was not observed for *Npm1-Alk*. Taken together, our data illustrate that lymphomas driven by the variant ATIC-ALK fusion (and likely by RNF213-ALK and TPM3-ALK), but not the classic NPM1-ALK, require an increased dosage of the *ALK* hybrid gene to compensate for the relatively low and insufficient expression and signaling properties of the chimeric gene.

Introduction

Anaplastic large cell lymphoma (ALCL) expressing ALK (ALK+ ALCL) is a rare but well-defined subtype of peripheral T-cell lymphoma (PTCL).[1] It accounts for approximately 3% of all non-Hodgkin lymphomas (NHL) in adults, 10-15% of pediatric lymphomas and 60-80% of all ALCLs. ALK+ ALCL is hallmarked by various 2p23/*ALK* chromosomal rearrangements leading to an aberrant expression and constitutive activation of the ALK tyrosine kinase. The most prevalent lesion occurring in more than 80% of ALK+ ALCL is t(2;5)(p23;q35) involving *ALK* and *NPM1*

Correspondence:
iwona.wlodarska@uzleuven.be

Received: March 24, 2016.
Accepted: June 26, 2017.
Pre-published: June 28, 2017.

doi:10.3324/haematol.2016.146571

Check the online version for the most updated information on this article, online supplements, and information on authorship & disclosures: www.haematologica.org/content/102/9/1605

(nucleophosmin) genes, respectively.[2] The translocation generates a chimeric protein comprising the N-terminal oligomerization domain of NPM1 and the C-terminal region of ALK, including its intracellular tyrosine kinase domain.[2] The fusion acts as an oncogene and its transforming potential was proven in a number of *in vitro* and *in vivo* studies.[3-5] The remaining ALK+ ALCL cases harbor variant 2p23/*ALK* rearrangements affecting at least nine partner genes: *TPM3* (1q21.3; previously assigned to 1q25),[6] *ATIC* (2q35), *TFG* (3q12.2), *TRAF1* (9q33.2), *CLTC* (17q23.1), *ALO17/RNF213* (17q25.3), *TPM4* (19p13.12), *MYH9* (22q12.3) and *MSN* (Xq12).[7] These partners play a key role in the constitutive activation of the chimeric protein by mediating its oligomerization and determining the subcellular localization of ALK fusion (cytoplasmic and nuclear in NPM1-ALK-positive cases, and cytoplasmic-only or membranous in variant fusions).[8,9] In addition, they impact a range of biological activities of ALK chimeras, including proliferation, transformation and metastatic capacities.[10,11] Comparative analysis of the biological properties of ALK oncoproteins, however, is hampered by the relative low-frequency of particular variant ALK fusions.

Interestingly, ALK rearrangements have also been detected in large B-cell lymphoma and various tumors of mesenchymal and epithelial origin, including inflammatory myofibroblastic tumors, lung cancer, esophageal squamous cell carcinoma and others.[7] Notably, the same ALK fusions, such as TPM3-ALK, TPM4-ALK, TFG-ALK, SEC31A-ALK, ATIC-ALK, CLTC-ALK and EML4-ALK occur in ALK+ malignancies of different cells of origin, highlighting the crucial role of ALK in tumorigenesis.[7,12] These findings prompted the development of new therapeutic strategies regarding ALK+ tumors. Of particular importance is the recent discovery of specific ALK tyrosine inhibitors,[13,14] one of which, crizotinib, has proven to have clinical efficacy in the treatment of ALK+ non-small cell lung cancer and ALCL.[15,16]

Herein, we report the molecular characterization of ALK fusions in eight ALK+ ALCL cases exhibiting a cytoplasmic-only ALK staining pattern recently diagnosed in our institution. Intriguingly, all cases analyzed by fluorescence *in situ* hybridization (FISH) at the time of diagnosis revealed copy number gain of the rearranged *ALK* gene.

Methods

Case selection

Eight cases of ALK+ ALCL with a cytoplasmic-only expression of ALK and available bioarchived material were selected from the database of the Center for Human Genetics and Department of Pathology, University Hospital Leuven, Belgium. Morphology, immunophenotype and clinical records of the reported cases were reviewed. The institutional review board "Commissie Medische Ethiek" of the University Hospital approved this retrospective study and renounced the need for written informed consent from the participants (S56799, ML10896: 12/08/2014).

Cytogenetics and FISH

Conventional Giemsa (G)-banding chromosomal analysis and FISH analysis followed routine protocols. The probes applied on patient material and Ba/F3 cell lines are listed in the *Online Supplementary Table S1*. Non-commercial probes were directly labeled with SpectrumOrange- and SpectrumGreen-dUTP (Abbott Molecular, Ottignies, Belgium) by random primed labeling. FISH images were acquired with a fluorescence microscope equipped with an Axiophot 2 camera (Carl Zeiss Microscopy, Jena, Germany) and a MetaSystems Isis imaging system (MetaSystems, Altlussheim, Germany).

Array-based genomic hybridization (aCGH)

Total genomic DNA was isolated from frozen lymphoma samples using standard procedures. High-resolution aCGH was performed using Affymetrix Cytoscan HD, following the manufacturer protocols. Downstream data analysis of copy number alterations was conducted using the software Array Studio, version 6.2.

Cell culture and growth curves

Ba/F3 cells constitutively expressing Cas9 (Ba/F3 Cas9) were generated using a retroviral expression vector containing a Cas9 expression cassette (*Online Supplementary Figure S1*). Ba/F3 Cas9 cells were cultured with interleukin 3 (IL3) in Roswell Park Memorial Institute (RPMI) medium + 10% fetal bovine serum (FBS) before and after electroporation. For growth curves, viability and proliferation were measured on a Guava flow cytometer (Merck Millipore, Darmstadt, Germany) for several consecutive days.

Quantitative real time polymerase chain reaction (QRT-PCR)

QRT-PCR with the GoTaq qPCR Master Mix (Promega, Madison, WI, USA) was used to analyze relative messenger ribonucleic acid (mRNA) expression of two *Alk* partner genes (*Npm1* and *Atic*) in Ba/F3 Cas9 cells. Mouse *Hprt1* and *Rpl4* were used as an internal control. Primers are listed in the *Online Supplementary Table S2*. All samples were run in triplicate and data were analyzed with the comparative Ct (ΔΔCt) method.

CRISPR/Cas genome editing

Guide (g)RNAs were designed using the Zhang lab's clustered regularly interspaced short palindromic repeats (CRISPR) design tool (Broad Institute of MIT and Harvard, Cambridge, MA, USA) (*Online Supplementary Table S3*). gRNAs were cloned into an expression plasmid (pX321, derived from pX330, Zhang lab; *Online Supplementary Figure S2*). Electroporations of Ba/F3 Cas9 cells were carried out using a Gene Pulser Xcell electroporation system (Bio-Rad Laboratories, Hercules, CA, USA). After electroporation, cells were kept in RPMI medium + 10% FBS + IL3 for three days before IL3 depletion was carried out.

Other applied techniques, including the 5' Rapid Amplification of Complementary (c)DNA ends (RACE) PCR, Low Coverage Full Genome Sequencing (LCFGS), Targeted Locus Amplification (TLA) and Nested RT-PCR are briefly described in the *Online Supplementary Methods*.

Results

Clinical and pathological features

Relevant clinical and pathological features of the reported cases of ALK+ ALCL are shown in Table 1. There were two children (a 5-year-old boy and a 13-year-old girl) and six adults (two female and four males) ranging from 49 to 78 years of age (mean 64.8 years). All patients presented with lymph node involvement and one displayed additional skin lesions (stages I [cases 3 and 4], II [cases 5 and 8], III [cases 2 and 7] and IV [cases 1 and 6]). Five adult patients (cases 2-6) were treated with the chemotherapy regimen cyclophosphamide, adriamycin, vincristine and

prednisone (CHOP), reached complete remission (CR) and are still alive. The sixth adult patient (case 7), initially diagnosed with classical Hodgkin lymphoma, was treated with doxorubicin, bleomycin, vinblastinea and dacarbazine (ABVD) and radiotherapy, and also reached CR. He relapsed very recently (after 165 months) and died due to disease-related complications after the third course of CHOP. Two other patients also experienced a more aggressive disease course: one (case 2) achieved a second CR following treatment with dexamethasone, cytarabine and cisplatin (DHAP), and the first pediatric patient (case 1) initially treated according to the ALCL99 protocol, experienced three relapses. The latter achieved CR after treatment with crizotinib and allogenic stem cell transplantation, but died 72 months after diagnosis due to severe graft-*versus*-host disease (GvHD) and respiratory failure. The second pediatric patient (case 8) received six cycles of polychemotherapy (ALCL99) and remains in CR.

Histopathology showed proliferation of anaplastic lymphoid cells and the presence of hallmark doughnut cells in all cases. The immunophenotype of the individual tumors is shown in Table 1 and illustrated in the *Online*

Table 1. Relevant clinical and pathological data.

Case	Sex/ Age at diagnosis	Sites of involvement, Ann Arbor stage	Immunophenotype	Histology	Treatment	Outcome	Survival (months)	Status (A/D)
1	M/5	Skin, supra and infradiaphragmatic lymph nodes. Stage IV.	CD3-, CD20-, CD30+, CD4 partial, CD8-, ALK(cyto)+ ,TIA1+, perforin +, granzyme B focal +	lymphohistiocytic subtype	Sequential polychemotherapy (ALCL99 protocol, high risk); 1st R: ALCL relapse protocol, BEAM + auto SCT; 2nd R: weekly vinblastine until 1.5 year; 3rd R: daily crizotinib + weekly vinblastine followed by MUD allo SCT	1st R 8 mo AD; 2nd R: 15 mo AD; 61 mo AD	72	D in CR (toxic death: severe GvHD, respiratory failure)
2	M/55	Lymph nodes (neck). Stage III.	CD3-, CD20-, CD30+, CD5-, CD10-, prekeratin-, EMA-, CD2-, CD4+, CD7-, CD8-, TIA1-, granzymB-, perforin+, ALK(cyto)+, EBV-, bcl2 weak+, CD43-	classical morphology of ALCL	8 CHOP; 1st R: 4 DHAP; BEAM + auto SCT	CR after CHOP; R: CR after DHAP	63	A
3	F/49	Lymph nodes (axillary). Stage I.	CD2-, CD3-, CD20-, PAX5-, CD15-, CD30+, CD4+, CD8-, CD5-, MUM1+, ALK(cyto)+, TIA1-, granzymeB-, perforin+, EBV-, EMA+	intrasinusoidal growth, numerous plasma cells and eosinophils in the background	N CHOP	CR	20	A
4	M/77	Lymph nodes (neck). Stage I.	CD2-, CD30+, CD4-, CD8-, ALK(cyto)+, TIA1-, granzymeB-, perforin+, EMA+, weak CD138, PAX5-, IgA-, HHV8-, CD7-, CD45-, CD79a-	classical morphology of ALCL, foci of necrosis; histiocytes in background	6 CHOP	CR	24	A
5	M/52	Lymph nodes (mesenteric). Stage IIA.	CD30+, CD4+, CD8-, ALK(cyto)+, TIA1+, perforin+, granzymeB+, EBV-,EMA+	large multinuclear cells with nucleoli; polymorphic stromal reactions with numerous plasma cells, neutrophils and eosinophils	8 CHOP	CR	45	A
6	F/78	Bone, supra and infra diaphragmatic lymph nodes. Stage IVB	CD30+, ALK (cyto)+, CD45+, CD4+, CD20 weak+, Pax5 weak+, CD3-, CD5-, CD2-, CD8- Perforin+, granzyme+, EMA+, TIA1-	classical morphology of ALCL	8 CHOP	CR	14	A

Table 1: continuation

7	M/65	Lymph nodes (neck, axillary, retoroperitoneal, iliacal). Stage IIIa.	CD30+, CD15 false +, CD20-, CD3-, misdiagnosed as classical Hodgkin. Performed in 2016 after recurrence: PAX5-, CD2-, CD4-, CD8-, ALK(cyto)+, TIA1+ (partial), perforin+, granzymeB+ (partial), EBV-	Nodular sheet-like proliferation of immunoblastic to anaplastic cells; prominent intrasinusoidal localization; similar at recurrence, plus prominent histiocytic response with erythrophagocytosis and emperipolesis	2002: (initially misdiagnosed as classical Hodgkin): 6 ABVD + RT at left cervical and axillar region (30 Gy). Relapse in February 2016: stadium IVB (neck, supra- and infradiaphragmatic lymph nodes, lung (subpleural lesions)). 8 CHOP (3 received).	R: 166 mo AD	168	D
8	F/13	Lymph nodes (infradiaphragmatic: retroperitoneal, iliacal). Stage IIA.	CD30+, ALK (cytoplasmic, membraneous) +, EMA+, TIA1+, perforin+, GranzymeB+, CD4+ (weak), CD20-, CD3-	Diffuse parenchymal and pseudo-cohesive intrasinusoidal spread of characteristic hallmark cells. No prominent stromal reaction.	ALCL 99 protocol: 6 courses of polychemotherapy	CR	14	A

M: male; F: female; R: relapse; SCT: stem cell transplantation; ABVD: doxorubicin, bleomycin, vinblastine, dacarbazine; CHOP: cyclophosphamide, adriamycin, vincristine, prednisone; DHAP: dexamethasone, cytarabine, cisplatin; BEAM: carmustine, etoposide, cytarabine, melphalan; MUD: matched unrelated donor; RT: radiotherapy; N: number of cycles unknown; CR: complete response; AD: after diagnosis; D: died; A: alive; GvHD, graft-*versus*-host disease; mo: months; cyto: cyoplasmic; ALCL: anaplastic large cell lymphoma.

Supplementary Figure S3. All cases were CD30 positive, expressed a CD4$^+$ or null cell phenotype in conjunction with variable cytotoxic markers, and overexpressed ALK1 in a strictly cytoplasmic pattern. The stromal infiltrate was prominent in all cases with a variable amount of histiocytes and/or neutrophils.

Cytogenetic and molecular studies

Case 1. Cytogenetic analysis showed a complex karyotype with del(2)(p23) (Table 2). FISH with LSI ALK demonstrated a break apart (BA) pattern with the green (5'*ALK*) signal on del(2)(p23) and two red (3'*ALK*) signals on a marker chromosome of postulated chromosome 11 origin (Figure 1A). Whole chromosome painting proved that der(11) indeed harbors the duplicated fragment of chromosome 2 inserted at 11q. The t(2p23/*ALK*) rearrangement was further investigated using the 5' RACE PCR approach. The analysis identified an in-frame fusion transcript in which exon 8 of *EEF1G*, the gene located at 11q12.3, was fused to exon 20 of *ALK* (Figure 1B). More precisely, the fusion joined nucleotide 1161 of *EEF1G* (The National Center for Biotechnology Information (NCBI) ref: NM-001404), corresponding to an intronic region between exons 8 and 9, with nucleotide 4226 of *ALK* (NM-004304) situated in exon 20. The *EEF1G-ALK* fusion was subsequently confirmed by Sanger sequencing of the fragment obtained by nested RT-PCR (Figure 1B) and by FISH using probes for 5'*EEF1G* and 3'*ALK* (*data not shown*). Array Comparative Genomic Hybridization (CGH) analysis demonstrated that 3'*ALK* is involved in the gain of 2p23.2p25.3 and that the gain of 11q11q13.4 affects *EEF1G* (Figure 1C,D). In addition, the gain of five other regions, loss of three large regions, including that of 9p21.3p24.3/*CDKN2A/B*, and three microdeletions were detected (Figure 1C; Table 1). Interestingly, the focal deletion at 8q24.21 covered ~280 kbp sequences flanking the centromeric border of *MYC*. The loss was confirmed by FISH with LSI MYC; one of two apparently normal looking chromosomes 8 [der(8)] revealed a significantly diminished red signal (Figure 1A).

Case 2. Cytogenetic analysis was unsuccessful. Interphase FISH with LSI ALK showed a BA pattern associated with the gain of up to seven red (3'*ALK*) signals (Figure 2A). The FISH pattern suggested a diploid and tetraploid status of abnormal cells. The *ALK* rearrangement was further investigated using LCFGS. The analysis identified the *RNF213-ALK* fusion (supported by at least eight read pairs) whereby exon 8 of *RNF213* is fused to exon 20 of *ALK*, resulting in an in-frame fusion transcript equal to the previously described cases (Figure 2B).[6,17,18] The fusion and its gain were confirmed by FISH (Figure 2A). The performed aCGH analysis demonstrated the *ALK*- and *RNF213*-associated gain of 2p23.2p25.3 and 17q23.3q25.3, respectively (Figure 2C,D). In addition, aCGH detected the gain of six other regions and loss of three regions, all listed in Table 2. Notably, breakpoints of the amplified 4p12p16 and 5q33.3q35.3 regions affected the *RNF212*/4p16 and *ITK*/5q33.3 genes, respectively. FISH with the respective BA probes (see *Online Supplementary Table S1*) confirmed the unbalanced rearrangement and partial gain of both genes. Furthermore, FISH with the probes for 5'*RNF212* and 3'*ITK* showed multiple, but not colocalized, signals, precluding the *RNF212-ITK* hybrid gene (*data not shown*). Unfortunately, LCFGS did not identify any fusion of *RNF212* and *ITK*.

Cases 3-6. The cases were not subjected to cytogenetic analysis. FISH with LSI ALK applied on formalin-fixed paraffin-embedded (FFPE) material confirmed ALK rearrangement and displayed the presence of three to seven red (3'*ALK*) signals in all cases (Table 2, Figure 3A). Although a number of fused (F), red (R) and green (G) signals in analyzed cells varied, all cases showed a clear predominance of the red signals and variations of the 1F1G3R

pattern. As a similar pattern was observed in ATIC-ALK-positive lymphoma,[19] we initially examined the status of this gene. FISH with the *ATIC* BA assay revealed a BA pattern and the presence of extra 5'*ATIC* signals in all four cases (Figure 3B). Subsequent FISH with the 5'*ATIC* and 3'*ALK* probes demonstrated three to five fused signals per cell, confirming the *ATIC-ALK* rearrangement and gain of the chimeric gene in all four cases (Figure 3C).

Case 7. The biopsy taken at time of relapse (2016) showed a complex diploid karyotype with a presumed der(1)ins(1;?)(q21;?) and ider(1)(q10) containing a duplicated 1q arm of der(1)ins(1;?)(q21;?) and del(2)(p23) (Table 2,

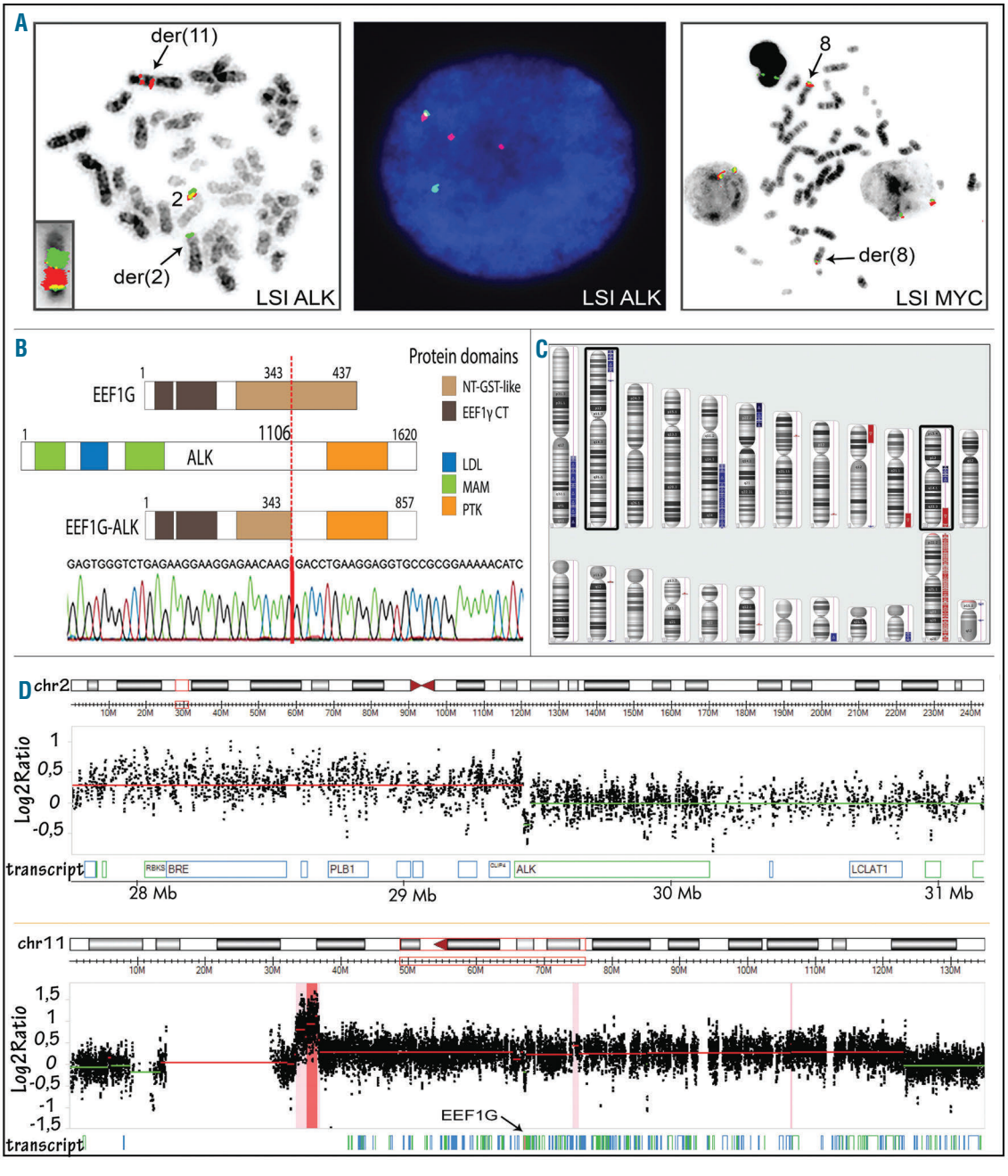

Figure 1. Cytogenetic and molecular analysis of case 1.(A) Examples of FISH experiments with LSI ALK and LSI MYC BA probes. Metaphase FISH demonstrated BA LSI ALK pattern associated with a duplication of the red/3'*ALK* signal on der(11) (left image). Paints for chromosomes 2 (red) and 11 (green) confirmed insertion of 2p23p25 at 11q12 (inset). The same aberrant LSI ALK pattern (one colocalized-one green-two red signals) was observed in interphase cells (middle image). Metaphase FISH with LSI MYC showed a diminished red signal on der(8), confirming a focal deletion at 8q24.21 (right image). (B) Schematic representation of the EEF1G, ALK and EEF1G-ALK protein structures (upper panel). Sequencing of the fragment amplified by *EEF1G-ALK* nested RT-PCR identified an in-frame fusion between exon 8 of *EEF1G* (breakpoint between exon 8 and 9) and exon 20 of *ALK* (breakpoint in the middle of exon 20) as shown in the electropherogram (lower panel). (C) Array CGH profile of case 1 showing several unbalanced regions, including gain of 2p23pter and 11q11q13.4 (marked). (D) The selected 2pter (upper panel) and 11q (lower panel) regions. Note the 2p23pter gain-associated break within the *ALK* gene (gain of 3'*ALK*) and localization of *EEF1G* in the middle of gained 11q11q13.4 region.

Figure 3D). Interphase FISH with LSI ALK revealed the 1F1G3R pattern (Figure 3E), as found in *ATIC-ALK*-positive cases. Considering that the 1q21 breakpoint merges with the localization of *TPM3*, the known partner of *ALK*,[6] a possible involvement of this gene was investigated by FISH with the designed *TPM3* BA assay (*Online Supplementary Table S1*). Neoplastic cells revealed the 1F3(RsepG) pattern, thus postulating the rearrangement of *TPM3* due to ins(1;2)(q21.3;p23p25) (Figure 3F). The *TPM3-ALK* fusion was subsequently confirmed by FISH using the 5'*TPM3*/3'*ALK* probes. In the proceeding step, we revised the diagnostic sample (the case was initially misdiagnosed as classical Hodgkin lymphoma), whereby cytogenetic analysis identified rare hypertetraploid cells with i(1)(q10) and del(2)(p23) (Table 2). FISH with LSI ALK (Figure 3G), *TPM3* BA (Figure 3H) and the 5'*TPM3*/3'*ALK*

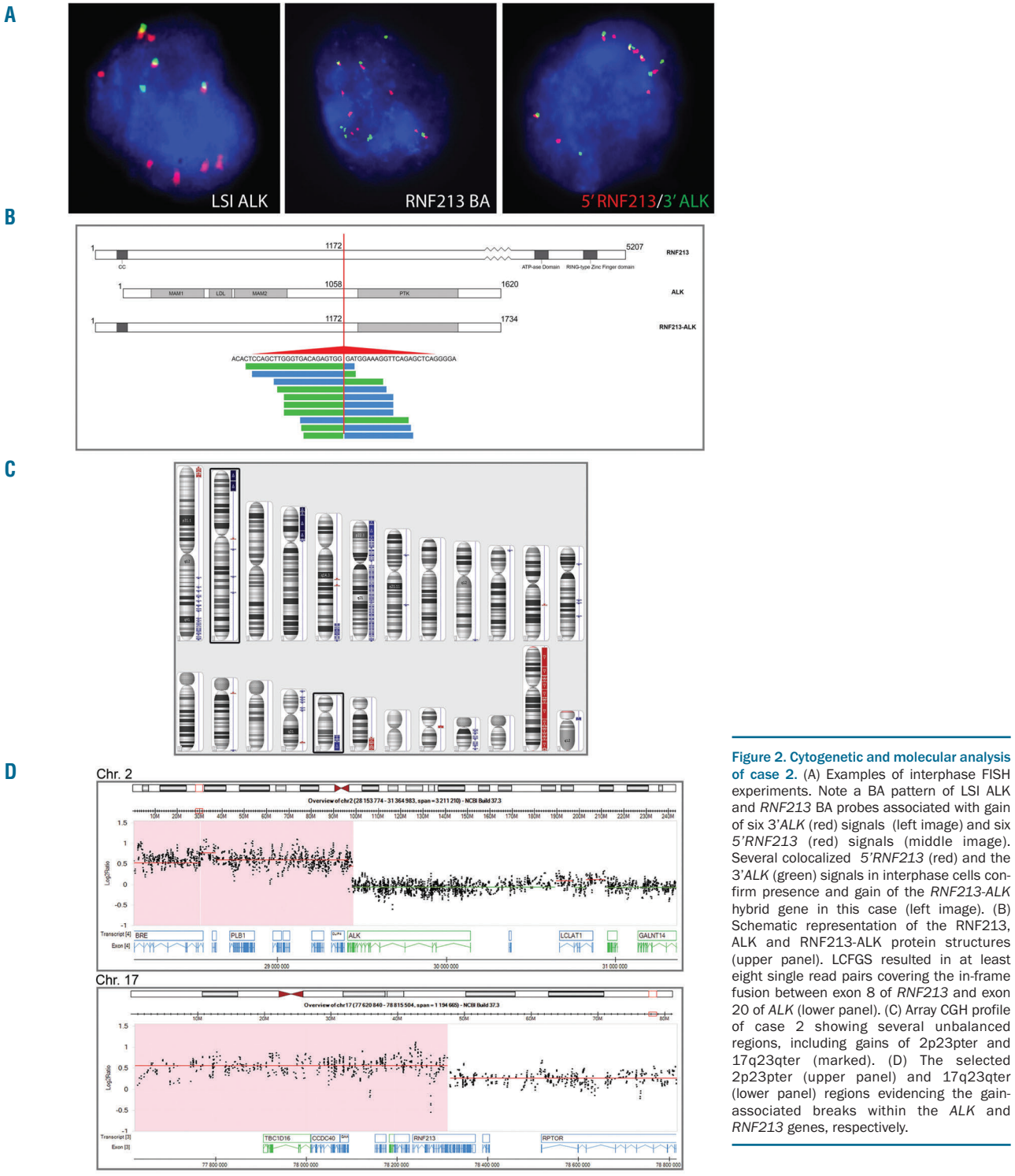

Figure 2. Cytogenetic and molecular analysis of case 2. (A) Examples of interphase FISH experiments. Note a BA pattern of LSI ALK and *RNF213* BA probes associated with gain of six 3'*ALK* (red) signals (left image) and six 5'*RNF213* (red) signals (middle image). Several colocalized 5'*RNF213* (red) and the 3'*ALK* (green) signals in interphase cells confirm presence and gain of the *RNF213-ALK* hybrid gene in this case (left image). (B) Schematic representation of the RNF213, ALK and RNF213-ALK protein structures (upper panel). LCFGS resulted in at least eight single read pairs covering the in-frame fusion between exon 8 of *RNF213* and exon 20 of *ALK* (lower panel). (C) Array CGH profile of case 2 showing several unbalanced regions, including gains of 2p23pter and 17q23qter (marked). (D) The selected 2p23pter (upper panel) and 17q23qter (lower panel) regions evidencing the gain-associated breaks within the *ALK* and *RNF213* genes, respectively.

probes (Figure 3I) demonstrated the presence, at the time of diagnosis (2002), of the *TPM3-ALK* rearrangement and copy number gain of the *ALK* fusion.

Case 8. Cytogenetic analysis identified only one abnormal (near tetraploid) metaphase cell harboring five copies of chromosome 2 (Table 2). LSI ALK applied on this metaphase cell hybridized with all chromosomes 2: one showed a fused signal and the other four were marked by red signals (Figure 3J). The abnormal FISH pattern (1-2F4R) was detected in 11% of interphase cells. Loss of the 5'*ALK* sequences suggested a focal interstitial del(2)(p23p23) leading to a novel fusion of *ALK* with a gene located at the centromeric breakpoint of the deletion. To identify a

Table 2. Results of cytogenetic and molecular studies.

Case	Sample/ status	Cytogenetics	aCGH profile	FISH LSI ALK	Other probes	ALK fusion partner gene (localization)	Detected by
1a	LN/P	44-47,XY,-Y,del(2)(p23),-5[3], der(6)t(5;6)(q22;p25),add(8)(p23)[3],-9, del(10)(q25),der(11)(?::11pter->q12.3::2p23-> 2pter::2pter->p23::11q12.3->q11::q13.5-> 23.1::?), add(12)(q24)[3],+16[2],+1-4mar[4]	gains: 1q21.3q44, 2p23.2p25.3, 5q15q35.3, 6p22.2p25,11q11q13.4, 22q13.1q13.33 20q13.1q13.33, losses: 8q24q24,9p21.3p24.3, 10q25.3q25, 11q22.3q25	ish: 2p(F),der(2)(G), der(11)(Rx2); nuc ish:1F,1G,2R (85%)	WCP2:2+,del(2p)+, der(11)+; WCP11:11+, der11+;5'EEF1G-SO/3'ALK-SG:2F1R1G; LSI MYC: 8F,8GRdim	*EEF1G* (11q12.3)	5'RACE PCR
2a	LN/D	NM	gains: 1q21.3q44, 2p23.2p25.3, 4p12p16, 5q33.3q35.3, 6, 12q15q23.2, 16p11.2p13.3, 17q23.3q25.3, 21q11.2q22.3 losses: 1p36.2p36.3, 5q15q21.2, 18q11.2q23	nuc ish:1-3F,1-3G, 1-7R (19%)	RFN213 BA:3F3-7R3-7G; 5'RFN213-SO/3'ALK-SG: 3-7F2-3R2-3G; RNF212 BA: 5-7GITK BA: 5-7R5'RNF SO/3'ITK-SG: 5-7R5-7G	*RFN213* (17q25.3)	LCFGS
3b	LN/D	ND	ND	nuc ish:1-2F,1-2G,5-7R (16%)	ATIC BA: variable pattern with gain of red signals; 5'ATIC-SO/3'ALK- SG: 2-5F and variable R/G signals	*ATIC* (2q35)	FISH
4b	LN/D	ND	ND	nuc ish: 1F,1G,5R (15%)	ATIC BA: variable pattern with gain of red signals; 5'ATIC-SO/3'ALK- SG: 2-5F and variable R/G signals	*ATIC* (2q35)	FISH
5b	LN/D	ND	ND	nuc ish:1-3F,1-2G,3-5R (21%)	ATIC BA: variable pattern with gain of red signals; 5'ATIC-SO/3'ALK- SG: 2-5F and variable R/G signals	*ATIC* (2q35)	FISH
6a	LN/D	NM	ND	nuc ish:1-2F,1-3G,3-5R (9%)	ATIC BA: variable pattern with gain of red signals; 5'ATIC-SO/3'ALK- SG: 2-5F and variable R/G signals	*ATIC* (2q35)	FISH (9%)
7a	LN/D	88-89,XXY,-Y,i(1)(q10),+i(1)(q10),del(2)(p11),+del(2)(p11),+del(2)(p23)x2, -4,-5,-8,-8,-11,-15,-15,-18,-18,+20[2], +20[2],-21,-22[2],+2-6mar[cp3]	ND	nuc ish:2-5F,1-2G, 5-6R (15%)	TPM3 BA: 1-2F5(RsepG); 5'TPM3-S0/3'ALK-SG: 1-2R1-3G5F	*TPM3* (1q21.3)	FISH
	LN/P	47,XY,ins(1;2)(q21.3;p23p25), +ider(1)(q10)ins(1;2)(q21.3;p23p25), del(2)(p23)[2]	ND	nuc ish:1F,1G,3R (24%)	TPM3 BA: 1F3(RsepG); 5'TPM3-S0/3'ALK-SG: 1R1G3F		
8	LN/D	88,XX,-X,-X,-1,add(1)(q44),+2, -3,add(4)(p16),+5,+7,-11,+12,-13,-15,-16,+i(17)(q10),-19,-20[1]	ND	2F,4xdel(2)(p23p?) Nuc ish:1F4R (11%)	TPM3 BA: 2F4R; 5'TPM3-S0/3'ALK-SG:2R1G4F	*TPM3* (1q21.3)	TLA

[a]FISH performed on cytogenetic specimen; [b]FISH performed on FFPE material. FISH: fluorescence *in situ* hybridization; aCGH: array-based comparative genomic hybridization; LN: lymph node; D: diagnosis; P: progression; NM: no mitosis, ND: not done; ish: *in situ* hybridization; nuc ish: interphase *in situ* hybridization; F: fused ; G: green; R: red; BA: break apart; RACE PCR: rapid amplification of cDNA ends polymerase chain reaction; LCFGS: low coverage full genome sequencing; TLA: targeted locus amplification technology.

potential partner gene, we used the TLA approach. Unexpectedly, the analysis identified the *TPM3-ALK* fusion with the breakpoints at the intron 7 of *TPM3* and the intron 19 of *ALK* (*Online Supplementary Figure S4*). FISH confirmed the *TPM3* rearrangement, which was associated with loss of the 3'*TPM3* sequences, and showed that four out of five chromosomes 2 harbor one copy of *TPM3-ALK* (Figure 3K,L). Altogether, we identified a cryptic insertion of the 5'*TPM3* into the rearranged *ALK* locus, loss of the 5'*ALK* and 3'*TPM3* sequences, and gain of two copies of *TPM3-ALK*.

Functional studies

Gain of the *EEF1G*-, *RFN213*-, *ATIC*- and *TPM3-ALK* hybrid genes found in the present cases contrasts with a constant occurrence of a single copy of *NPM1-ALK* in t(2;5)-positive ALCL.[20-22] We hypothesized that ALCLs harboring the variant rearrangements compensate an insufficient expression of the *ALK* fusions (driven by relatively weak promoters of the partner genes) *via* an increased dosage of the chimeric gene. To validate this concept, we analyzed expression levels of *NPM1, EEF1G, RNF213, ATIC* and *TPM3* in various normal lymphoid

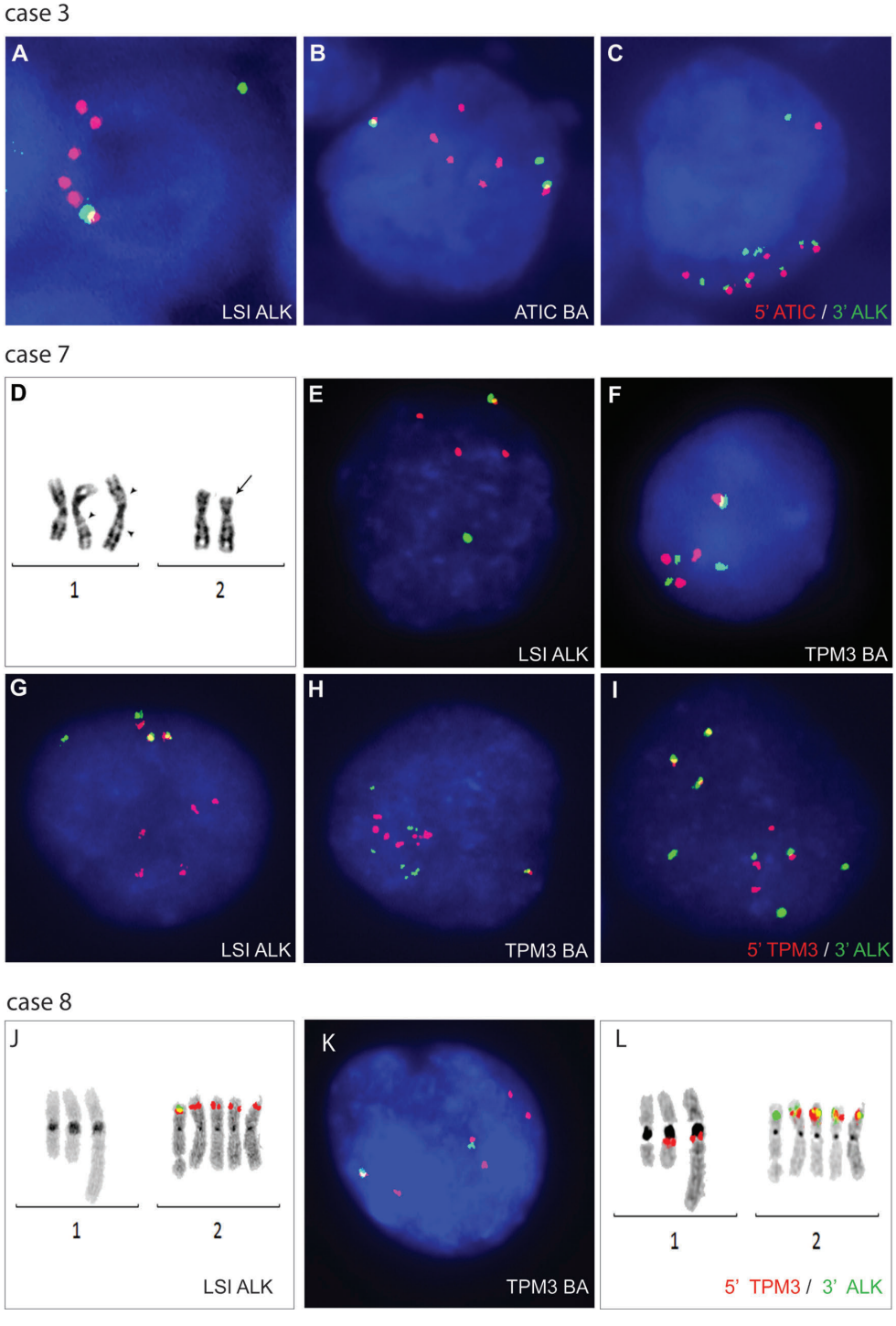

Figure 3. Cytogenetic and FISH analysis of cases 3, 7 and 8. (A-C) Note a BA pattern of LSI ALK and ATIC BA probes associated with a gain of four 3'*ALK* (red) and four 5'*ATIC* (red) signals, respectively, in case 3. Several colocalized 5'*ATIC*/3'*ALK* signals in interphase cells demonstrate gain of the *ATIC-ALK* hybrid gene in this sample. Similar FISH results were obtained in cases 4 and 5. Case 7: (D) Partial karyotype (at time of relapse) illustrating insertion of 2p23p25 at 1q21.3 (arrowhead), isochromosome 1q containing duplicated long arm of ins(1;2)(q21.3;p23q25) (two arrowheads) and del(2)(p23) (arrow). (E) Note rearrangement of *ALK* and gain of two extra 3'*ALK* (red) signals, and (F) three separated red and green *TPM3* BA probes, likely marking ins(1) and ider(1). (G-I) Similar FISH patterns were observed in the diagnostic sample. Case 8: (J) Note four copies of der(2) marked by red signals of LSI ALK, (K) unbalanced rearrangement of *TPM3* and (L) loss of *TPM3* from one chromosome 1 and four copies of der(2)/*TPM3-ALK*.

cells and T-cell malignancies using previously generated RNA sequencing (Seq) data.[23,24] The analysis revealed a significantly lower (*P*-value <0.001) expression of *RNF213*, *ATIC* and *TPM3* in all samples when compared to *NPM1* (Figure 4A). In contrast, expression of *EEF1G* was similar to that of *NPM1*. Based on these findings, we hypothesized that oncogenic transforming properties of the three variant ALK fusions, RFN213-ALK, ATIC-ALK and

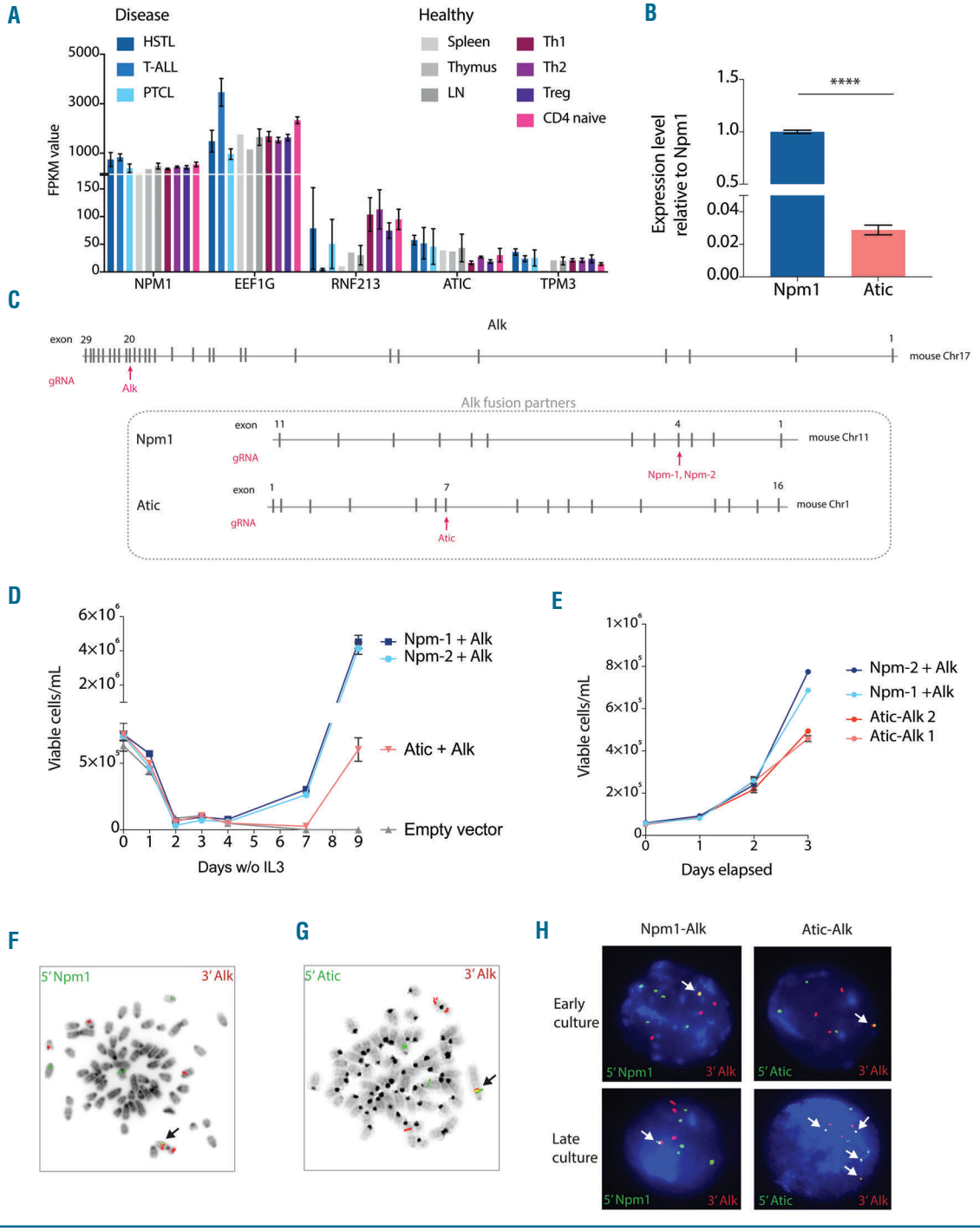

Figure 4. Functional analysis of the NPM1-, EEF1G-, RNF213-, TPM3- and ATIC-ALK fusions. (A) Expression analysis of the five *ALK* partner genes using previously generated RNA-Seq data.[23,24] In contrast to *EEF1G*, expression of *TPM3, RNF213,* and *ATIC* is significantly lower (*P*-value <0.001) when compared to *NPM1* in different malignant and non-malignant cell types (HSTL: hepatosplenic T-cell lymphoma [n=4]; T-ALL: T-cell acute lymphoblastic leukemia [n=5]; PTCL: peripheral T-cell lymphoma [n=2]; Spleen [n=1]; Thymus [n=1]; LN: lymph nodes [n=3]; Th1: T helper 1 cells [n=5]; Th2: T helper 2 cells [n=5]; Treg [n=5], and CD4 naïve T-cells [n=4]). Error bars represent the standard deviation (SD). (B) QRT-PCR on Ba/F3 Cas9 cells showing the expression levels of *Npm1* and *Atic*. The expression of *Atic* is significantly lower than *Npm1* (*P*<0.001). Error bars represent the SD. (C) Representation of the *Alk, Npm1,* and *Atic* mouse genes. Exons are indicated by vertical bars. Red arrows indicate the location of the gRNA target sites. (D) Growth curve showing the transforming capacities of Ba/F3 Cas9 cells harboring an endogenous *Npm1-Alk* or *Atic-Alk* fusion. Error bars represent the SD. (E) Growth curve showing the growth rate of Ba/F3 Cas9 cells after transformation by the endogenous Alk fusion. Error bars represent the SD. (F-H) Examples of metaphase and interphase FISH results showing the endogenous Alk fusions in Ba/F3 Cas9 cells. Arrows indicate colocalized signals/chimeric genes. Note a constant presence of a single copy of *Npm1-Alk* and gain of *Atic-Alk* in late cultures. w/o: without; IL3: interleukin 3.

TPM3-ALK, could be lower than the strong NPM1-ALK kinase. To validate our hypothesis, we attempted to generate the Npm-Alk and Atic-Alk fusions in the genome of Ba/F3 cells using CRISPR/Cas9 genome editing. The expression level of *Npm1* is around 50-fold higher than the expression level of *Atic* in this cell line, making it a suitable model to test our hypothesis (Figure 4B). We designed a gRNA targeting exon 20 of *Alk* and gRNAs targeting *Npm1* and *Atic* in regions corresponding to the breakpoints observed in our patient samples (Figure 4C). gRNAs targeting *Alk* and a fusion partner were simultaneously introduced in Ba/F3 Cas9 cells by electroporation. Upon IL3 depletion, both endogenous Alk fusions were able to transform the Ba/F3 Cas9 cells, although cells harboring an endogenous Atic-Alk fusion needed more time to recover from this depletion (Figure 4D). In addition to the slower transformation rate, cells harboring an endogenous Atic-Alk fusion presented with a lower growth rate after transformation than cells with an endogenous Npm1-Alk fusion (Figure 4E). FISH demonstrated the presence of one copy of the *Npm1-Alk* and *Atic-Alk* chimeric genes per cell in the respective cell lines (Figure 4F,G). After keeping the cells in culture for three months, we observed gain of one to three copies of the *Atic-Alk* fusion gene in approximately 20% of these cells. In contrast, the *Npm1-Alk* cell line kept a single copy of the chimeric gene in all cells (Figure 4H). Altogether, these data demonstrate that the Npm1-Alk fusion is a more potent driver of proliferation than Atic-Alk in Ba/F3 cells, and that the expression level of the fusion partner is a key factor in the transformation potential of the oncogenic fusions.

Discussion

Our study provided evidence that ALCL driven by at least three variant ALK fusions, RNF213-ALK, ATIC-ALK and TPM3-ALK, is characterized by a copy number gain of the *ALK* hybrid gene. Gain of *RNF213-ALK* was already observed by us in the previously reported case of ALK+ ALCL, harboring two copies of der(17)t(2;17)(p23.2;q25.3)/*RNF213*(*ALO17*)-ALK.[17] Genetic mechanisms underlying the amplification of *RNF213-ALK* in case 2, however, remain unknown. Notably, the four ATIC-ALK-positive cases presented herein, as well as all reported ATIC-ALK cases documented by FISH,[19,25-27] showed extra copies of the chimeric gene. We previously documented that the *ATIC-ALK* fusion is generated by a pericentric inv(2)(p23q35) and is constantly accompanied by isochromosome 2q [derivative of inv(2)] comprising two extra copies of *ATIC-ALK*.[19,25] Based on these data, we presume that the cases reported herein also carry inv(2)(p23q35) and one to three copies of ider(2q). Intriguingly, a similar mechanism of gain of *ALK* hybrid emerged to underpin the *TPM3-ALK* rearrangement detected in case 7. The fusion was likely created by the insertion of 3'*ALK*/2p23p25 at 1q21.3/*TPM3* and gained by a subsequent formation of ider(1)(q10). In the second *TPM3-ALK*-positive case, however, the chimeric gene was produced by a cryptic insertion of 5'*TPM3* into the rearranged *ALK* locus and gained by a duplication of the der(2), as in the case reported by Siebert *et al.*[28] Notably, one more informative case with *TPM3-ALK* also presented with two to three copies of the 3'*ALK*.[29] Lamant *et al.*,[6] who originally described the *TPM3-ALK* fusion in ALK+ ALCL, linked it to t(1;2)(q25;p23). Considering, however, an opposite transcriptional orientation of both genes, generation of the in-frame *TPM3-ALK* fusion requires more complicated events, as illustrated in the present and previously reported cases.[28]

Altogether, our genetic findings, supported by the published data,[17,19,26-29] highlight a strong association of *RNF213-ALK, ATIC-ALK* and *TPM3-ALK* with a copy number gain of the chimeric gene. A spectrum of such ALK fusions is probably broader, but a frequent lack of cytogenetic and/or FISH data hampers their identification. These observations contrast with ALCL driven by *NPM1-ALK*[20-22] and at least three variant fusions, *CLTC-ALK*,[17] *TPM4-ALK*[30,31] and *TRAF1-ALK*,[27,32] shown to carry a single copy of the *ALK* hybrid gene. We initially included the novel *EEF1G-ALK* variant found to be duplicated on der(11) in the former category. Given, however, that two recently published ALCL cases with *EEF1G-ALK* did not show copy number gain of the *ALK* fusion gene,[33] duplication of *EEF1G-ALK* in our case was likely associated with progression of the disease, similar to a case of leukemic ALK+ ALCL with an extra copy of *NPM1-ALK*.[34] This conclusion is additionally supported by our other data illustrating a strong expression of *EEF1G* in normal and malignant T cells, similar to that of *NPM1*. Thus, there is no reason why the *EEF1G-ALK* fusion gene would require an increased copy number.

In contrast, expression of *RNF213, ATIC* and *TPM3* in lymphoid cells was significantly lower than *NPM1* and *EEF1G*. These findings support the concept that ALCL driven by the *RNF213-ALK, ATIC-ALK* and *TPM3-ALK* fusions might require an increased dosage of the *ALK* chimeric gene to compensate an insufficient expression of ALK in neoplastic cells. To test if the best documented ATIC-ALK fusion is indeed less transforming than the NPM1-ALK fusion, we generated the *Npm1-Alk* and *Atic-Alk* fusion genes by inducing Cas9 mediated chromosomal rearrangements in Ba/F3 cells. Growth properties of these engineered cells showed that the transformation potential of *Atic-Alk* is significantly lower when compared to *Npm1-Alk*, likely due to a lower expression level of *Atic*. Interestingly, the tendency of the Atic-Alk-positive Ba/F3 cells to gain extra copies of the *Atic-Alk* chimeric gene recapitulates the events observed in the original tumors and confirms the selective pressure of the cells to acquire additional copies of the *Atic-Alk* fusion. We also attempted to generate an endogenous *Rnf213-Alk* fusion, but since *Rnf213* is very lowly expressed in Ba/F3 cells, this fusion could not transform the cells. *Tpm3* was not included in the functional studies, since it was only recently added to the study. Of note, Giuriato *et al.*[35] previously showed that in conditional knock-in mice both TPM3-ALK and NPM1-ALK could induce B-cell lymphoma/leukemia with a similar disease latency. In these transgenic mice, however, the expression levels of both ALK fusions were similar, since their expression was driven by an external promoter. This could explain the observed equal tumorigenic potential of both ALK fusions.

The novel *EEF1G-ALK* fusion which we identified in a child with ALK+ ALCL extends the already long list of *ALK* fusion partners comprising approximately 20 genes.[7] The very recent report of two pediatric patients with *EEF1G-ALK*[33] indicates that the fusion is recurrent and strongly associated with pediatric ALK+ ALCL. *EEF1G*, located at 11q12.3, has 10 exons encoding for an eukaryotic translation elongation factor 1γ. Together with α, β

and δ subunits, it forms the eukaryotic elongation factor complex, which is predominantly involved in protein biosynthesis with an elongation of the polypeptide chains.[36,37] EEF1G comprises a glutathione-S-transferase (GST)-like N-terminal domain and a C-terminal (CT) domain.[37] Although all four subunits of the elongation factor complex are highly expressed in most eukaryotic cells, the role of human EEF1G is poorly understood. Notably, an increased expression of EEF1G has been detected in various human carcinomas.[37-40] It has been suggested that overexpression of EEF1G stimulates the overgrowth of neoplastic cells.[41] In the present case of ALK+ ALCL, exons 1 to 8 of *EEF1G* are fused to exon 20-29 of *ALK*, resulting in a chimeric protein with the complete GST-like N-terminal domain and part of the CT domain of EEF1G, fused to the complete intracellular protein tyrosine kinase (PTK) domain of ALK (Figure 2B). Even though the complete PTK domain is involved, the ALK fragment contains the final 513 amino acids, which is shorter in comparison to the fragment involved in most other ALK fusions, containing the final 563 amino acids.[42] Of note, both cases reported by Palacios *et al.*[33] revealed breakpoints within intron 7 of *EEF1G* and intron 20 of *ALK*. As the fusions were identified by RNA-Seq, genetic mechanisms underlying these rearrangements are unknown.

The postulated t(2;11)(p23;q12.3), however, is unlikely due to an opposite transcriptional orientation of both genes, similar to *TPM3* and *ALK*. Functional studies performed by the authors provided evidence of the dimerization properties of the EEF1G-ALK fusion, constitutive activation of ALK kinase and its strong oncogenic potential similar to that of NMP1-ALK.

Our patient with *EEF1G-ALK* experienced an unfavorable and fatal clinical course. Although ALK+ ALCL has a relatively good prognosis, chemoresistant and aggressive forms of this lymphoma, recurrently featured by *MYC* aberrations, have been recurrently reported.[32,43-45] Notably, our case displayed a microdeletion neighboring *MYC* and loss of *CDKN2A/B* at 9p21, a known poor prognostic factor in tumors.[46] We presume that a focal del(8)(q24q24) could activate *MYC* by loss of negative regulatory elements upstream of the gene, for example. Although clinical data of the EEF1G-ALK-positive cases reported by Palacios *et al.*[33] are not available, we believe that an aggressive clinical course and unfavorable prognosis of certain ALK+ ALCL is not determined by the type of *ALK* fusion, but rather by secondary hits affecting potent oncogenes and tumor suppressor genes (e.g., *MYC, TP53, PRDM1* and *CDKNA2/B*).[32,44,45,47]

In summary, we investigated eight recently diagnosed cases of ALK+ ALCL with a cytoplasmic-only expression of ALK and identified one novel *EEF1G-ALK* rearrangement and three already known fusions, *RNF213-ALK*, *TPM3-ALK* and *ATIC-ALK*. Occurrence of the latter rearrangement in four out of eight (50%) of the cases studied confirms that *ATIC-ALK* is the most prevalent variant fusion in ALK+ ALCL. Importantly, *RNF213-ALK*, *TPM3-ALK* and *ATIC-ALK* fusions were recurrently present in two or more copies, contrasting with the *NPM1-ALK* chimeric gene which constantly occurs in one copy. Our functional studies show that ALK+ ALCL driven by *ATIC-ALK* compensates the weak expression and possibly weak oncogenic properties of this variant ALK fusion by an increased gene dosage. We propose a similar explanation for the copy number gain of *RNF213-ALK* and *TPM3-ALK*. Altogether, our findings support the hypothesis that the transforming capacities of ALK fusions depend on the biological features of the partner genes.[48]

Acknowledgments

The authors would like to thank Vanessa Vanspauwen and Emilie Bittoun for their excellent technical assistance, and Rita Logist for the editorial help.

Funding

This study was supported by the concerted action grant from the KU Leuven no. 3M040406 (JAvdK, PV, TT, JC and IW), research grants from the FWO Vlaanderen (G081411N to TT) and "Stichting tegen Kanker" (PV). MVDB holds a SB Fellowship of the Research Foundation-Flanders. PV is a senior clinical investigator of the FWO-Vlaanderen. TT holds a Mandate for Fundamental and Translational Research from the "Stichting tegen Kanker" (2014-083).

References

1. Swerdlow SH, Campo E, Harris NL, et al. WHO classification of tumours of haematopoietic and lymphoid tissues. 4th ed. Lyon, France: International Agency for Research on Cancer: 2008.
2. Morris SW, Kirstein MN, Valentine MB, et al. Fusion of a kinase gene, ALK, to a nucleolar protein gene, NPM, in non-Hodgkin's lymphoma. Science. 1994;263(5151):1281-1284.
3. Chiarle R, Gong JZ, Guasparri I, et al. NPM-ALK transgenic mice spontaneously develop T-cell lymphomas and plasma cell tumors. Blood. 2003;101(5):1919-1927.
4. Kuefer MU, Look aT, Pulford K, et al. Retrovirus-mediated gene transfer of NPM-ALK causes lymphoid malignancy in mice. Blood. 1997;90(8):2901-2910.
5. Lange K, Uckert W, Blankenstein T, et al. Overexpression of NPM-ALK induces different types of malignant lymphomas in IL-9 transgenic mice. Oncogene. 2003; 22(4):517-527.
6. Lamant L, Dastugue N, Pulford K, Delsol G, Mariame B. A new fusion gene TPM3-ALK in anaplastic large cell lymphoma created by a (1;2)(q25;p23) translocation. Blood. 1999;93(9):3088-3095.
7. H Hallberg B, Palmer RH. Mechanistic insight into ALK receptor tyrosine kinase in human cancer biology. Nat Rev Cancer. 2013;13(10):685-700.
8. Falini B, Pileri S, Zinzani PL, et al. ALK+ lymphoma: clinico-pathological findings and outcome. Blood. 1999;93(8):2697-2706.
9. Boi M, Zucca E, Inghirami G, Bertoni F. Advances in understanding the pathogenesis of systemic anaplastic large cell lymphomas. Br J Haematol. 2015;168(6):771-783.
10. Drexler HG, Gignac SM, von WR, Werner M, Dirks WG. Pathobiology of NPM-ALK and variant fusion genes in anaplastic large cell lymphoma and other lymphomas. Leukemia. 2000;14(9):1533-1559.
11. Stein H, Foss Hd, Du H, et al. CD30+ anaplastic large cell lymphoma : a review of its histopathologic, genetic, and clinical features. Blood. 2000;96(12):3681-3695.
12. Sakamoto K, Nakasone H, Togashi Y, et al. ALK-positive large B-cell lymphoma: identification of EML4-ALK and a review of the literature focusing on the ALK immunohistochemical staining pattern. Int J Hematol. 2016;103(4):399-408.
13. Mologni L. Inhibitors of the anaplastic lymphoma kinase. Expert Opin Investig Drugs. 2012;21(7):985-994.
14. Pall G. The next-generation ALK inhibitors. Curr Opin Oncol. 2015;27(2):118-124.
15. Kwak EL, Bang YJ, Camidge DR, et al. Anaplastic lymphoma kinase inhibition in non-small-cell lung cancer. N Engl J Med. 2010;363(18):1693-1703.
16. Gambacorti PC, Farina F, Stasia A, et al. Crizotinib in advanced, chemoresistant anaplastic lymphoma kinase-positive lymphoma patients. J Natl Cancer Inst. 2014; 106(2):djt378.

17. Cools J, Wlodarska I, Somers R, et al. Identification of novel fusion partners of ALK, the anaplastic lymphoma kinase, in anaplastic large-cell lymphoma and inflammatory myofibroblastic tumor. Genes Chromosomes Cancer. 2002;34(4):354-362.
18. Hernandez L, Bea S, Bellosillo B, et al. Diversity of genomic breakpoints in TFG-ALK translocations in anaplastic large cell lymphomas: identification of a new TFG-ALK(XL) chimeric gene with transforming activity. Am J Pathol. 2002;160(4):1487-1494.
19. Wlodarska I, De Wolf-Peeters C, Falini B, et al. The cryptic inv(2)(p23q35) defines a new molecular genetic subtype of ALK-positive anaplastic large-cell lymphoma. Blood. 1998;92(8):2688-2695.
20. Mathew P, Sanger WG, Weisenburger DD, et al. Detection of the t(2;5)(p23;q35) and NPM-ALK fusion in non-Hodgkin's lymphoma by two-color fluorescence in situ hybridization. Blood. 1997;89(5):1678-1685.
21. Perkins SL, Pickering D, Lowe EJ, et al. Childhood anaplastic large cell lymphoma has a high incidence of ALK gene rearrangement as determined by immunohistochemical staining and fluorescent in situ hybridisation: a genetic and pathological correlation. Br J Haematol. 2005; 131(5):624-627.
22. Cataldo KA, Jalal SM, Law ME, et al. Detection of t(2;5) in anaplastic large cell lymphoma: comparison of immunohistochemical studies, FISH, and RT-PCR in paraffin-embedded tissue. Am J Surg Pathol. 1999;23(11):1386-1392.
23. Finalet Ferreiro J, Rouhigharabaei L, Urbankova H, et al. Integrative genomic and transcriptomic analysis identified candidate genes implicated in the pathogenesis of hepatosplenic T-cell lymphoma. PloS One. 2014;9(7):e102977.
24. Atak ZK, Gianfelici V, Hulselmans G, et al. Comprehensive analysis of transcriptome variation uncovers known and novel driver events in T-cell acute lymphoblastic leukemia. PLoS Genet. 2013; 9(12):e1003997.
25. Ma Z, Cools J, Marynen P, et al. Inv(2)(p23q35) in anaplastic large-cell lymphoma induces constitutive anaplastic lymphoma kinase (ALK) tyrosine kinase activation by fusion to ATIC, an enzyme involved in purine nucleotide biosynthesis. Blood. 2000;95(6):2144-2149.
26. Colleoni GW, Bridge JA, Garicochea B, Liu J, Filippa DA, Ladanyi M. ATIC-ALK: A novel variant ALK gene fusion in anaplastic large cell lymphoma resulting from the recurrent cryptic chromosomal inversion, inv(2)(p23q35). Am J Pathol. 2000; 156(3):781-789.
27. Takeoka K, Okumura A, Honjo G, Ohno H. Variant translocation partners of the anaplastic lymphoma kinase (ALK) gene in two cases of anaplastic large cell lymphoma, identified by inverse cDNA polymerase chain reaction. J Clin Exp Hematop. 2014;54(3):225-235.
28. Siebert R, Gesk S, Harder L, et al. Complex variant translocation t(1;2) with TPM3-ALK fusion due to cryptic ALK gene rearrangement in anaplastic large-cell lymphoma. Blood. 1999;94(10):3614-3617.
29. Hoshino A, Nomura K, Hamashima T, et al. Aggressive transformation of anaplastic large cell lymphoma with increased number of ALK-translocated chromosomes. Int J Hematol. 2015;101(2):198-202.
30. Meech SJ, McGavran L, Odom LF, et al. Unusual childhood extramedullary hematologic malignancy with natural killer cell properties that contains tropomyosin 4--anaplastic lymphoma kinase gene fusion. Blood. 2001;98(4):1209-1216.
31. Liang X, Meech SJ, Odom LF, et al. Assessment of t(2;5)(p23;q35) translocation and variants in pediatric ALK+ anaplastic large cell lymphoma. Am J Clin Pathol. 2004;121(4):496-506.
32. Abate F, Todaro M, van der Krogt J, et al. A novel patient derived tumorgraft model with TRAF1-ALK anaplastic large cell lymphoma translocation. Leukemia. 2014;(6):1-32.
33. Palacios G, Shaw TI, Li Y, et al. Novel ALK fusion in anaplastic large cell lymphoma involving EEF1G, a subunit of the eukaryotic elongation factor-1 complex. Leukemia. 2017;31(3):743-747.
34. Ries S, Rnjak L, Mitrovic Z, Kuvezdic KG, Nola M, Sucic M. CD13+ anaplastic large cell lymphoma with leukemic presentation and additional chromosomal abnormality. Diagn Cytopathol. 2010;38(2):141-146.
35. Giuriato S, Foisseau M, Dejean E, et al. Conditional TPM3-ALK and NPM-ALK transgenic mice develop reversible ALK-positive early B-cell lymphoma/leukemia. Blood. 2010;115(20):4061-4070.
36. Kumabe T, Sohma Y, Yamamoto T. Human cDNAs encoding elongation factor 1 gamma and the ribosomal protein L19. Nucleic Acids Res. 1992;20(10):2598.
37. Achilonu I, Siganunu TP, Dirr HW. Purification and characterisation of recombinant human eukaryotic elongation factor 1 gamma. Protein Expr Purif. 2014;99:70-77.
38. Chi K, Jones DV, Frazier ML. Expression of an elongation factor 1 gamma-related sequence in adenocarcinomas of the colon. Gastroenterology. 1992;103(1):98-102.
39. Ender B, Lynch P, Kim YH, Inamdar NV, Cleary KR, Frazier ML. Overexpression of an elongation factor-1 gamma-hybridizing RNA in colorectal adenomas. Mol Carcinog. 1993;7:18-20.
40. Lew Y, Jones DV, Mars WM, Evans D, Byrd D, Frazier ML. Expression of elongation factor-1 gamma-related sequence in human pancreatic cancer. Pancreas. 1992;7:144-152.
41. Mimori K, Mori M, Inoue H, et al. Elongation factor 1 gamma mRNA expression in oesophageal carcinoma. Gut. 1996;38(1):66-70.
42. Van Roosbroeck K, Wlodarska I. Oncogenic anaplastic lymphoma kinase rearrangements in lymphoma. European Haematology. 2009;3:50-56.
43. Moritake H, Shimonodan H, Marutsuka K, Kamimura S, Kojima H, Nunoi H. C-MYC rearrangement may induce an aggressive phenotype in anaplastic lymphoma kinase positive anaplastic large cell lymphoma: Identification of a novel fusion gene ALO17/C-MYC. Am J Hematol. 2011; 86(1):75-78.
44. Liang X, Branchford B, Greffe B, et al. Dual ALK and MYC rearrangements leading to an aggressive variant of anaplastic large cell lymphoma. J Pediatr Hematol Oncol. 2013; 35(5):e209-e213.
45. Monaco S, Tsao L, Murty VV, et al. Pediatric ALK+ anaplastic large cell lymphoma with t(3;8)(q26.2;q24) translocation and c-myc rearrangement terminating in a leukemic phase. Am J Hematol. 2007; 82(1):59-64.
46. LaPak KM, Burd CE. The molecular balancing act of p16(INK4a) in cancer and aging. Mol Cancer Res. 2014;12(2):167-183.
47. Boi M, Rinaldi A, Kwee I, et al. PRDM1/BLIMP1 is commonly inactivated in anaplastic large T-cell lymphoma. Blood. 2013;122(15):2683-2693.
48. Armstrong F, Duplantier MMl, Trempat P, et al. Differential effects of X-ALK fusion proteins on proliferation, transformation, and invasion properties of NIH3T3 cells. Oncogene. 2004;23(36):6071-6082.